Nanotechnology **19** (2008) 332001 (14pp) doi:10.1088/0957-4484/19/33/332001

TOPICAL REVIEW

Recent progress in carbon nanotube-based gas sensors

Ting Zhang, Syed Mubeen, Nosang V Myung[1] and Marc A Deshusses[1]

Department of Chemical and Environmental Engineering, Center for Nanoscale Science and Engineering, University of California-Riverside, Riverside, CA 92521, USA

E-mail: myung@engr.ucr.edu and mdeshuss@engr.ucr.edu

Received 25 February 2008, in final form 4 June 2008
Published 7 July 2008
Online at stacks.iop.org/Nano/19/332001

Abstract

The development of carbon nanotube-(CNTs-)based gas sensors and sensor arrays has attracted intensive research interest in the last several years because of their potential for the selective and rapid detection of various gaseous species by novel nanostructures integrated in miniature and low-power consuming electronics. Chemiresistors and chemical field effect transistors are probably the most promising types of gas nanosensors. In these sensors, the electrical properties of nanostructures are dramatically changed when exposed to the target gas analytes. In this review, recent progress on the development of different types of CNT-based nanosensors is summarized. The focus was placed on the means used by various researchers to improve the sensing performance (sensitivity, selectivity and response time) through the rational functionalization of CNTs with different methods (covalent and non-covalent) and with different materials (polymers and metals).

(Some figures in this article are in colour only in the electronic version)

1. Introduction

The detection of biological and chemical species in atmosphere or process gases is of a great concern in relation to environmental pollution, industrial emission monitoring and process control, medical diagnosis, public security, agriculture and a variety of industries. The development of miniature and portable gas sensors that are able to detect gas analytes in real time with good sensing performance will significantly impact our daily life. Nanoengineered materials including one-dimensional nanostructures (e.g. nanowires, nanobelts, nanotubes and nanoribbons) hold great promise for the development of miniaturized chemical and biological sensors because of (1) greater adsorptive capacity due to large surface area to volume ratio, (2) greater modulation of electrical properties (e.g. capacitance, resistance) upon exposure to analytes [1] due to a greater interaction zone (i.e. Debye length) over the cross-sectional area (figure 1), (3) ability to tune electrical properties of the nanostructure by adjusting the composition and size and (4) the ease of configuration as chemiresistors and field effect transistors (FETs) and potential integration with low-power microelectronics to form complete systems with microprocessor and wireless communication units.

The discovery of carbon nanotubes (CNTs) in 1991 by Ijima [2] has generated great interest among researchers to explore their unique electrical, physical, mechanical and chemical properties to develop high performance devices. Researchers have been exploring the potential of CNTs in a wide range of applications: nanoelectronics, sensors, field emission, displays, hydrogen storage, batteries, polymer matrix composites, nanoscale reactors and electrodes [3–6]. Due to the distortion of the electron clouds of CNTs from a uniform distribution in graphite to asymmetric distribution around cylindrical nanotubes, a rich π-electron conjugation forms outside of the CNTs, making them electrochemically

[1] Address for correspondence: Department of Chemical and Environmental Engineering, University of California-Riverside, Bourns Hall, Riverside, CA 92521, USA.

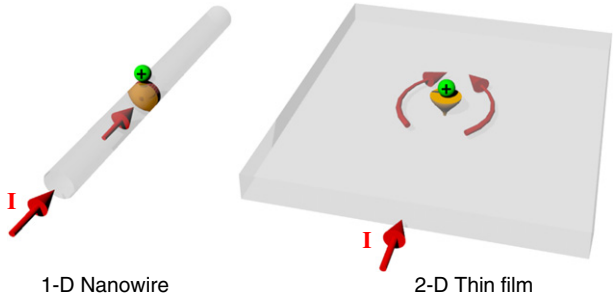

Figure 1. Schematic illustration of analyte and sensing material interaction. The orange (online) regions and green (online) ovals represent depletion depths and charged analytes, respectively. Binding to a 1D nanostructure leads to depletion/accumulation in the bulk of the nanostructure as opposed to only the surface in 2D sensors.

active [7]. The electrical properties of CNTs are extremely sensitive to charge transfer and chemical doping effects by various molecules. When electron-withdrawing molecules (e.g. NO_2, O_2) or electron-donating molecules (e.g. NH_3) interact with the p-type semiconducting CNTs, they will change the density of the main charge carriers (i.e. holes) in the 'bulk' of the nanotube, which changes the conductance of CNTs. This behavior forms the basis for applications of CNTs as electrical chemical gas sensors. However, gas sensors based on pristine CNTs have certain limitations, such as sometimes low sensitivity to analytes for which they have low adsorption energy or low affinity, lack of selectivity, or irreversibility or long recovery time. To overcome these limitations, several research groups are currently working on the functionalization of CNTs with different materials to alter their chemical nature and enhance their sensing performance.

2. Relevant carbon nanotubes' properties

CNTs are graphene sheets of covalently bonded carbon molecules rolled into hollow cylinders [8]. There are two main types of carbon nanotubes: single-walled carbon nanotubes (SWNTs) which have a single carbon layer with a diameter of 1–5 nm and multi-walled carbon nanotubes (MWNTs) which have multiple layers of carbon (with an interlayer spacing of 3.4 Å) that are concentrically nested together [8]. Most of CNTs are synthesized by arc discharge, laser ablation or chemical vapor deposition [9–13].

Even though CNTs are composed of covalently bonded carbon, they exhibit an extreme diversity in structure–property relationships [8, 14–17]. SWNTs can be either semiconducting or metallic depending on the tube diameter and chirality [15, 16]. Semiconducting SWNTs are p-type semiconductors with holes as the main charge carriers. Semiconducting SWNTs have bandgap energies inversely related to their diameter; for a typical diameter of 1.4 nm, the bandgap is around 0.5 eV [8]. MWNTs have metallic electronic properties similar to metallic SWNTs. Due to the 1D structure, the electronic transport in metallic SWNTs and MWNTs behaves ballistically without scattering over long length. This property allows CNTs to carry high currents (up to 10^9 A cm^{-2}) with negligible heating [14].

3. Pristine CNT gas sensor

3.1. CNT chemiresistor and chemical field effect transistor (ChemFET)

CNTs are composed entirely of surface atoms, which is ideal for the direct electrical detection of trace chemical vapors where SWNTs act as both sensing materials and transducer. In the past several years, two different configurations, i.e. chemiresistor and back-gated chemical field effect transistor (ChemFET), have been employed for most CNT-based gas sensors to transduce analyte concentration directly into an electrical signal (figure 2).

In the chemiresistor configuration, a single CNT or mesh of CNTs is bridging the positive and negative electrodes through which current is passing (figure 2(a)). The binding of analytes on the CNT surface results in charge transfer

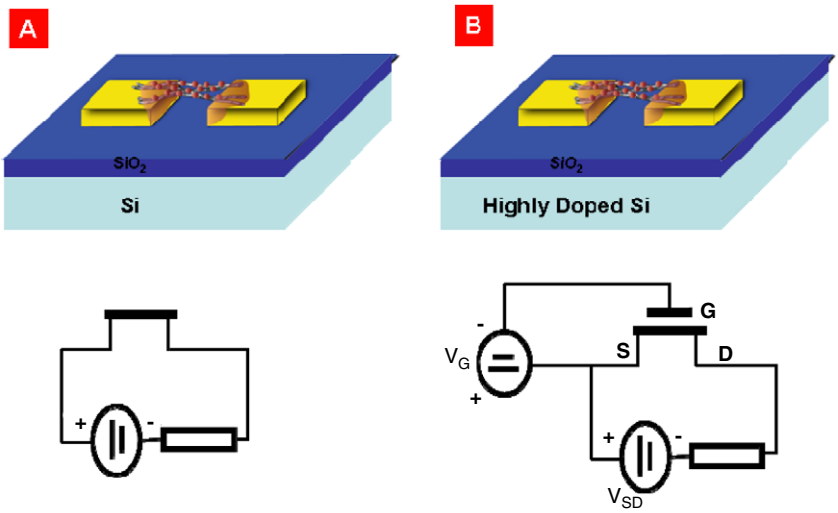

Figure 2. Schematic of chemiresistor (A) and ChemFET (B) configurations with functionalized CNTs contacting the two electrodes and with a highly doped silicon back gate (G) and a load resistor for the FET. S: source; D: drain; V_G: gate bias potential; V_{SD}: source–drain potential.

between the adsorbate and the surface of the CNT and alters its electrical resistance. The back-gated ChemFET configuration is similar to the chemiresistor except that the conductance of the CNT between source and drain is modulated by a third (i.e. gate) electrode capacitively coupled through a thin dielectric layer, usually a SiO_2 layer (see figure 2(b)) [18]. The semiconducting nanotubes connected by source and drain metal electrodes form a metal/semiconducting nanotubes/metal system, which exhibits p-type transistor characteristics. In general, ChemFETs tend to be more sensitive than chemiresistors because of the ability to tune the conductance of CNTs by controlling the gate voltage. This makes ChemFETs ideal candidates for electrically based sensing, although the ChemFETs require slightly more complex ancillary electronics than direct chemiresistors.

3.2. Methods to integrate CNTs into chemiresistor and ChemFET

Currently, there are mainly two methods to position CNTs across electrodes. One is to directly grow CNTs on the sensor platform via controlled chemical vapor deposition (CVD). The other is to drop-cast a CNT suspension or solution in water or in an organic solvent on top of prefabricated electrodes. The latter is sometimes followed by alignment or post-processing of the CNTs.

The growth of CNTs on the sensor platform with CVD methods involves heating catalytic metal nanoparticles to high temperatures (500–1000 °C) in a furnace, and feeding a hydrocarbon gas (e.g. ethylene, acetylene or methane) for a period of time [19]. Iron, cobalt or nickel nanoparticles are often used as the catalysts. They are usually patterned on a support platform such as a silicon substrate with silicon dioxide as the insulating layer, or on a porous aluminum oxide substrate [19]. For MWNT growth, the growth temperature range is typically 550–750 °C, while the temperature required to form SWNTs is the range of 850–1000 °C. To form the electrode contacts with the CNTs, electrodes can be fabricated either by sputtering, evaporating or photolithographically patterning metal contacts such as gold pads over a single CNT or over a CNT network. CNTs can also be grown via CVD across prefabricated electrodes. In both cases, fabrication methods are complex and the yields are low. Inexpensive, high yield and reproducible fabrication techniques are essential for the success of CNT-based sensors.

Recent advances in carbon nanotube chemistry enable both the dissolution and dispersion of CNTs in various solvents [20]. These provide new alternative routes for fabricating CNT patterns by simply dispensing/printing the dissolved/dispersed particles on substrates. The sensor electrical resistance, which is dependent on the density of CNTs across the electrode contacts, can simply be tuned by adjusting the concentration of the CNTs in the dispersion or by adjusting the dispensed volume. In addition to drop-casting of CNTs using microsyringes, screen printing, inkjet printing and air brushing have been used sometimes followed by dielectrophoresis (DEP) to align the CNTs across the electrodes. Compared to the CVD-grown single SWNT-based sensor, these methods are more reproducible, cost effective, manufacturable and have higher yields.

Very little differences exist between the methods of fabrication for chemiresistors and ChemFETs. While the substrates for ChemFETs should allow for back gate configuration, most fabrication methods described above will work for both chemiresistor and ChemFET configurations. Ancillary electronic equipment will, of course, be quite different between ChemFETs and chemiresistors, the latter requiring much simpler and cheaper electronics.

3.3. Fabrication and sensing performance of pristine CNT chemiresistor and ChemFET

In 2000, Dai and coworkers first demonstrated that single semiconducting SWNTs can act as fast and sensitive ChemFETs at ambient temperatures [21]. They fabricated individual semiconducting SWNT ChemFETs by growing SWNTs via CVD on SiO_2/Si substrates, then photolithographically patterning Ti/Au pads over a single SWNT for electrical contact (i.e. source and drain). The metal/semiconducting SWNT/metal system exhibited p-type transistor characteristics with several orders of magnitude change in conductance under various gate voltages. Upon exposure to NO_2 and NH_3, the conductance of the semiconducting SWNT changed dramatically. An increase in the conductance by three orders of magnitude was observed within several seconds when exposed to 200 ppm NO_2 ($V_g = +4$ V), while the conductance decreased about two orders of magnitude within two minutes when exposed to 10 000 ppm NH_3 ($V_g = 0$ V) (figure 3).

Similar ChemFETs were tested with different alcohol vapors with good reversibility and reproducibility by Someya *et al* [22]. The semiconducting SWNTs were synthesized by CVD and the electrode contacts were formed by evaporating Au with metal shadow masks. When exposed to several saturated vapors of methanol, ethanol, 1-propanol, 2-propanol and tert-butanol with $V_g = -20$ V and $V_{sd} = -100$ mV, the response time was within 5–15 s. Collins *et al* and other researchers found the conductance of nanotubes is sensitive to ambient environments, especially to O_2 and oxygen-containing gaseous species [23].

Novak *et al* demonstrated that a ChemFET sensor based on a SWNT network can detect dimethyl methylphosphonate (DMMP), a simulant for the nerve agent Sarin [24]. The sensors were reversible and capable of detecting DMMP at sub-ppb concentration levels ($V_g = 0$ V). A fast recovery (a few minutes) of the sensor was achieved by applying +3 V gate bias after exposure. The recovery was accelerated by the Coulombic interaction between the negative charge induced by the positive gate bias and DMMP which is a strong electron donor. Similar recovery using back gate bias was observed by Chang *et al* [25] who found that a negative back gate voltage was required to refresh SWNT ChemFET sensors exposed to ammonia and that a positive voltage was required to refresh sensors exposed to NO_2. They suggested that this effect could be used to partly circumvent the low sensing specificity of pristine SWNT sensors and allow for a better identification of analytes.

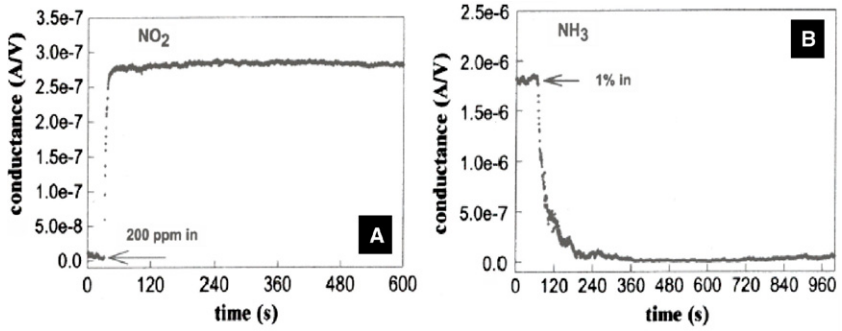

Figure 3. Electrical conductance response of a semiconducting SWNT to (A) 200 ppm NO_2 and (B) 1% NH_3 vapor. (From Kong *et al* [21] reprinted with permission from AAAS.)

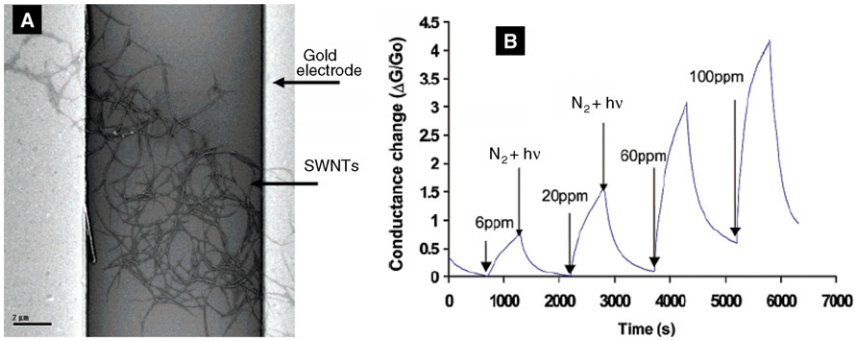

Figure 4. (A) SEM image of SWNTs across two gold electrodes. (B) Representative sensor response to NO_2 and recovery after UV light exposure. (Adapted with permission from Li *et al* [27]. Copyright 2003 American Chemical Society.)

Valentini *et al* fabricated chemiresistor sensors based on CNT mats [26]. CNT mats were deposited by plasma-enhanced CVD on Si_3N_4/Si substrates, with prefabricated platinum interdigitated electrodes on the top of Si_3N_4 to make electrode contact with the deposited CNTs. An integrated platinum heater on the back of the silicon substrate was used to control the sensor operating temperature. The sensor could detect NO_2 at concentrations as low as 10 ppb at the optimal operating temperature of around 165 °C.

Li *et al* fabricated a SWNT-based chemiresistor by drop-casting SWNTs dispersed in dimethylformamide (DMF) onto prefabricated interdigitated gold electrodes (IDEs) (figure 4) [27]. The SWNTs formed a network or a mesh on the IDEs after evaporation of the DMF. The sensors were tested for NO_2 and nitrotoluene at room temperature. Their responses were linear from ppb to ppm levels, with detection limits of 44 ppb for NO_2 and 262 ppb for nitrotoluene. The response time was a few minutes while the recovery to the baseline was much slower but was greatly accelerated by using UV irradiation.

Suehiro *et al* fabricated an ammonia sensor based on MWNT networks using dielectrophoresis (DEP) [28]. DEP is the electrokinetic motion of dielectrically polarized materials in non-uniform electric fields. The advantage of the DEP method is that the number of CNTs trapped in the region of interest can be controlled by the DEP force (e.g. frequency, amplitude) and by the duration of DEP trapping. MWNTs dispersed in ethanol were trapped and enriched in an interdigitated microelectrode gap using DEP. The authors investigated the changes in impedance in response to exposure to 10 ppm NH_3. Measurements were conducted at a frequency of 100 kHz and 8 V AC bias at room temperature. The sensor conductance decreased dramatically, while the capacitance increased in the presence of ammonia. Lee *et al* fabricated metallic SWNT-based sensors using dielectrophoretic alignment after drop-casting of a suspension of SWNTs [29]. The sensors exhibited an increase in the conductance when exposed to thionyl chloride ($SOCl_2$, a nerve agent precursor) and dimethylmethylphosphonate (DMMP, a nerve agent simulant), but the response was irreversible. They claimed that the signal transduction was mainly through the larger-diameter metallic nanotubes. The mechanism was proven by selective Raman decay showing an increase in the occupied density of states at the Fermi level of the metallic SWNTs after exposure to $SOCl_2$.

Kordás *et al* developed a potentially cost-effective inkjet printing for generating conductive MWNT patterns on paper and polymer surfaces [30]. They used a commercial desktop inkjet printer (Canon BJC 4550) to form the conductive pattern. The conductive pattern was found to be sensitive to very high concentrations of various gases or vapors such as H_2O, NH_3 and alcohols.

Wongwiriyapan *et al* demonstrated detection of O_3 with SWNT networks grown by CVD on a prefabricated sensor platform [31]. The sensor platform was an alumina substrate with interdigitated Pt electrodes (width: 50 μm, gap size:

50 μm) on the top and a Pt heater at the bottom. The sensors could detect ozone down to 6 ppb at room temperature, and a fast recovery time (a few minutes) was achieved by heating with the integrated heater until the sensor conductance had reverted to the baseline. The sensitivity was improved by initially using an electrical breakdown technique which consisted of applying a high voltage (15–60 V) between the Pt electrodes to selectively burn some of the metallic SWNTs in the network.

For pristine CNT sensors, the binding energy of the target gas analytes is usually large so that the analyte only slowly desorbs from the CNTs after the sensor is exposed to an analyte-free atmosphere. As will be discussed later, functionalization of CNTs has a significant effect on the binding energy and therefore on the dynamic response of CNT-based sensors. Experiments showed that NH_3 donates about 0.04 electron per molecule to SWNTs [32], while NO_2 withdraws approximately 0.1 electron per molecule with binding energy of 0.8 eV [33]. To accelerate the recovery process for restoring the initial conductance of CNT sensors, an external energy source may be implemented to rapidly desorb strongly adsorbed analytes by lowering the adsorption energy barrier. This can be achieved by local heating of the nanotubes to high temperatures ($\sim$200 °C), or using photo-induced desorption, such as ultraviolet light illumination [34]. It has been demonstrated by several researchers that UV light (250 nm) at low photon flux causes rapid desorption of adsorbed species from the SWNTs at room temperature. Photo-induced desorption is a non-thermal process, which is mainly due to electronic excitation of SWNTs.

3.4. Role of defects and dopants in CNT gas sensors

There are a few experimental and theoretical studies indicating that the sensitivity of CNT sensors can be improved by doping the CNTs or by introducing defect sites along the sidewall of the CNTs during the purification (oxidation) process. Valentini *et al* fabricated CNT thin film sensors based on defective and defect-free nanotube structures [35]. The transition from defect-free to defective CNTs can be induced through high temperature exposure to reactive plasma. Chemiresistors made with defective CNTs exhibited a greater sensitivity toward NO_2 compared to defect-free sensors. This observation was consistent with theoretical calculations indicating that the defect sites on the CNTs resulted in a strong chemisorption of NO_2 and a large charge transfer interaction, while the defect-free CNTs had a very weak interaction and negligible charge transfer. This is mainly due to the strong sp^2 carbon–carbon molecular bonding within CNTs which renders defect-free CNTs less sensitive to gas molecule bonding. Robinson *et al* observed that chemiresistive- and chemicapacitive-based SWNT sensors had a greater sensitivity toward various analytes (e.g. acetone, methanol, H_2O, hexane, toluene) by introducing carboxylic acid sites (<2% of the total sites) on the SWNTs [36] by exposing them to UV/O_3 followed by treatment in a H_2O_2 solution. They hypothesized that the greater sensing response might be caused by increased adsorbate binding energy and charge transfer at the defect sites. Watts *et al* reported on the response of MWNTs and acid-treated (3:1 H_2SO_4/HNO_3 mixture) MWNT chemiresistors to H_2O and O_2 [37]. Increased resistance for both types of sensors was observed when exposed to water vapor, while acid-treated MWNT sensors showed a higher sensitivity (5% relative resistance increase after 100 s exposure to humid air) compared to that of untreated MWNTs (3% relative resistance increase after 100 s exposure to humid air). This effect was explained by the formation of hydrogen bonds from polar water molecules with oxygen-containing defects on the MWNTs. This reduced the electron-withdrawing power of the oxygen-containing defect groups, thus increasing the density of holes in the MWNTs thereby increasing the electrical resistance. Similar enhancement of sensing was observed for the sensing of CO. Pristine SWNT-based sensors were not sensitive to CO because of the low affinity of CO for pristine SWNTs. To improve sensing performance, Peng *et al* [38] and Wang *et al* [39] proposed to dope SWNTs with B, N or Al or create $B_xC_yN_z$ ternary nanotubes. Based on *ab initio* calculations, they predicted that the sensitivity toward CO could be improved and controlled by adjusting the dopant level. Subsequently, Fu *et al* [40] demonstrated experimentally that sensors made with carboxylated SWNTs were sensitive to CO, with a lower detection limit of 1 ppm, whereas pristine SWNTs did not respond. The authors exploited the different responses of carboxylated and pristine SWNTs to differentiate between CO, NO and NO_2. Table 1 summarizes sensing performance of selected pristine CNT chemiresistors and ChemFETs.

3.5. Other types of CNT sensors

Snow *et al* demonstrated the use of SWNTs as chemicapacitors for sensing of both polar and non-polar gas molecules at room temperature [41]. The SWNT-based chemicapacitors were fabricated by a CVD-grown SWNT network on a 250 nm thick thermally grown silicon oxide on a highly doped silicon substrate. The capacitance was measured at 30 kHz and 0.1 V AC bias between the SWNTs and the heavily doped silicon substrate with 250 nm thick SiO_2. Under the applied bias, strong fringing electric fields radiate outward from the SWNTs surface and the polarization of the adsorbates can be detected as an increase in capacitance. This capacitance change was fast ($\sim$4 s response time), sensitive, completely reversible, and with low electrical noise. This approach enables detection of a wide range of analytes including less polar chemical vapors such as dimethyl formamide (DMF) and DMMP (figure 5). In follow-up work from the same group, both the capacitance and the conductance of the SWNT network were found to produce a rapid response (20 s) to high concentrations (>20 000 ppm) of various chemical vapors such as DMMP and acetone [42]. The responses were explained by the combination of two physico-chemical properties of adsorbates: polarizability and charge transfer. A remarkable finding was that the ratio of the capacitance change to the conductance change was concentration-independent and was an intrinsic property of the given analyte. This has potential application for the identification of unknown compounds.

Table 1. Summary of selected sensing performance of pristine CNT chemiresistors and ChemFETs. (Note: N/S = Not-stated.)

CNT type	Sensor configuration	Targeted analytes	Detection limit	Response time (s)	Reversibility	Reference
Single SWNT	ChemFET	NO_2, NH_3	2 ppm (NO_2) 0.1% (NH_3)	<600	Irreversible	Kong *et al* [21]
SWNTs	ChemFET	Alcoholic vapors (methanol, ethanol, 1-propanol, 2-propanol, and tert-butanol.)	N/S	5–150	Reversible (−20 V gate bias potential)	Someya *et al* [22]
SWNTs	Chemiresistor	O_2	N/S	N/S	Reversible	Collins *et al* [23]
SWNTs	ChemFET	DMMP	<1 ppb	1000	Reversible (3 V gate bias)	Novak *et al* [24]
MWNTs	Chemiresistor	NO_2	10 ppb	N/S	Reversible (165 °C)	Valentini *et al* [26]
SWNTs	Chemiresistor	NO_2, Nitrotoluene	44 ppb (NO_2), 262 ppb (Nitrotoluene)	600	Reversible (UV)	Li *et al* [27]
MWNTs	Chemiresistor	NH_3	10 ppm	∼100	Reversible	Suehiro *et al* [28]
SWNTs	Chemiresistor	$SOCl_2$, DMMP	100 ppm	10	Irreversible	Lee *et al* [29]
SWNTs	Chemiresistor	O_3	6 ppb	<600	Reversible	Wongwiriyapan *et al* [31]
MWNTs	Chemiresistor	NO_2	5–10 ppb	∼600 (165 °C)	Reversible (165 °C)	Valentini *et al* [35]
SWNTs	Chemiresistor	methanol, acetone	N/S	∼100	N/S	Robinson *et al* [36]
SWNTs	Chemiresistor	H_2O	N/S	10–100	Reversible	Watts *et al* [37]
Carboxylated SWNT	Chemiresistor	CO	1 ppm	∼100	Reversible	Fu *et al* [40]

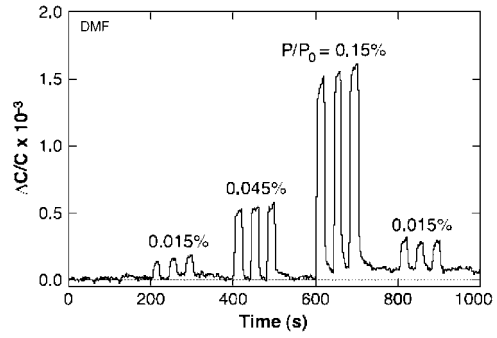

Figure 5. Measured relative capacitance change of a SWNT chemicapacitor in response to repeated 20 s pulses of dimethyl formamide (DMF) at varying concentrations. (From Snow *et al* [41] reprinted with permission from AAAS.)

Gas ionization sensors based on MWNTs have been developed by Modi *et al* [43]. The sensors were fabricated with a vertically grown MWNT anode on an SiO_2 substrate grown by CVD with aluminum as the cathode. The electrodes were separated by an approximately 180 μm thick glass insulator. The dimensions of the MWNTs were approximately 25–30 nm in diameter, 30 μm in length and 50 nm separation between the nanotubes. By applying a high voltage between electrodes, gases were ionized at the tips of MWNTs due to the high and nonlinear electric fields created near the tips. The breakdown voltage and the self-sustaining discharge current were specific to the nature of the gas analyte and its concentration. The sensor performance was not affected by various environmental conditions (temperature, moisture and gas flow).

A CNT microwave resonant sensor was developed by Chopra *et al* [44]. A resonant sensor undergoes a shift in resonant frequency upon exposure to various gaseous analytes. The CNT resonator sensors were fabricated from a circular disc electromagnetic resonant circuit coated with SWNTs or MWNTs. The downshift of resonant frequency when exposed to NH_3 was measured by a radio-frequency receiver. The results showed that SWNT- and MWNT-coated sensors had a response time of about 10 min, and had similar sensitivity toward NH_3 at concentrations ranging from 100 to 400 ppm. SWNT-coated sensors had a greater dynamic range than MWNTs which is consistent with their greater adsorption capacity of ammonia.

Ong *et al* developed a wireless, passive MWNT-SiO_2 composite-based gas sensor to detect CO_2, O_2 and NH_3 [45]. The sensing principle is based on changes of relative permittivity (ε) and conductivity (ε'') of the MWNT–SiO_2 composite placed on the interdigital space of a planar inductor–capacitor resonant circuit (LC) when exposed to various gases. The sensor resonant frequency was remotely monitored through a loop antenna. Cycling between pure nitrogen, oxygen and CO_2 resulted in rapid and reversible responses. Exposure to pure NH_3 resulted in partially irreversible responses attributed to the non-reversible chemisorption of NH_3 onto the MWNTs.

Penza *et al* fabricated surface acoustic wave (SAW) sensors which were coated with SWNTs and MWNTs to detect volatile organic compounds (VOCs) such as ethanol, ethylacetate and toluene [46]. They observed that CNT-coated SAW sensors have higher sensitivity (i.e. up to 3–4 orders of magnitude) than that of existing organic-layer-coated SAW at room temperature. The same group also demonstrated coating of SWNTs onto quartz crystal microbalance (QCM) and standard silica optical fiber (SOF) sensors for alcohol detection. The sensing mechanism is mainly due to changes in the mass and refractive index due to gas analyte adsorption.

4. Functionalized CNT gas sensors

Some of the potential drawbacks of using pristine CNTs as sensing elements are the lack of specificity to different gaseous analytes and the low sensitivity towards analytes that have no affinity to CNTs. These shortcomings can be, at least in part, circumvented by functionalizing the CNTs with analyte-specific entities. Functionalization also sometimes affects the sensor dynamics. There are two main approaches for the surface functionalization of CNTs: covalent functionalization and non-covalent functionalization, depending on the types of linkages of the functional entities onto the nanotubes. Currently, most covalently functionalized CNTs are based on esterification or amidation of carboxylic acid groups that are introduced on defect sites of the CNTs during acid treatment [47–49].

Non-covalent functionalization is mainly based on supramolecular complexation using various adsorptive and wrapping forces, such as van der Waals and π-stacking interactions, without destruction of the physical properties of CNTs [50, 51]. For example, Star *et al* demonstrated that poly-{(m-phenylenevinylene)-co-[(2,5-dioctyloxy-p-phenylene)-vinylene]} (PmPV) can be used for the wrapping around SWNTs by mixing SWNTs and PmPV in $CHCl_3$ with π–π stacking and van der Waals interactions between PmPV and the surfaces of the SWNTs [50]. Xia *et al* found that polymer-encapsulated MWNTs can be prepared through ultrasonically initiated *in situ* polymerizations of n-butyl acrylate (BA) and methyl methacrylate (MMA) in the presence of MWNTs [51]. Dong *et al* used thiolated heme modified SWNT networks for CO sensing at room temperature with the detection limit of 4.9 ppm [52]. They observed a greater sensitivity toward CO when using Cr instead of Au as the electronic contact pad, leading to the hypothesis that, in this case, CO sensing was mainly from the Cr–SWNT interface.

In terms of gas sensing with functionalized CNTs, much of the recent research has been directed toward nanostructures with either organic polymers or catalytic metal nanoparticles. The recent advances in these fields are reviewed in the following sections.

4.1. Organic polymer functionalized CNT gas sensors

Organic polymers have been used in gas sensors for more than two decades [53]. They react to analytes by changing their physical (e.g. volume changes upon exposure) or chemical (e.g. oxidation state) properties. Among the organic polymers, conducting polymers are the most promising materials for gas sensing as they have delocalized bonds that make them semiconducting or even highly conductive. Delocalization is accomplished by forming a conjugated backbone of alternating single and double bonds [54]. These new-generation polymers are particularly interesting because they exhibit the electronic, magnetic and optical properties of metals or semiconductors while retaining the attractive mechanical properties and processing advantages of polymers. Several conducting polymers (e.g. polyaniline, polypyrrole, polythiophene) have been demonstrated to be good sensing materials. They have been applied as conductometric, potentiometric, amperometric and voltammetric transducers for the detection of ammonia, nitrogen dioxide, carbon monoxide and VOCs. The conductance changes observed in the conducting polymers upon exposure to analytes is due to the redox interaction of electronically active analytes either with the polymer backbone itself or with the dopant molecules incorporated within the polymers, thereby modulating the doping level, charge mobility and/or the density of free charge carriers available [54]. Recently, enhanced gas sensing by combining SWNTs with organic polymers has been demonstrated.

There have been several reports on the development of gas sensors based on non-covalently functionalized SWNTs with organic polymers made by drop-coating or dip-coating methods. Qi *et al* showed that non-covalently drop-coating of polyethyleneimine (PEI) and Nafion (a polymeric perfluorinated sulfonic acid ionomer) onto SWNT ChemFETs resulted in gas sensors with improved sensitivity and selectivity for NO_2 and NH_3 [33]. The PEI functionalization changed the SWNTs from p-type to n-type semiconductors, and sensors were able to detect less than 1 ppb NO_2 while being insensitive toward NH_3. In contrast to PEI-coated sensors, Nafion-coated SWNTs were insensitive to NO_2 while exhibiting a good sensitivity toward NH_3 (figure 6). Star *et al* also fabricated non-covalently functionalized SWNT ChemFETs by simply submerging nanotube network FETs in an aqueous solution of PEI and starch overnight [55]. PEI–starch polymer-coated SWNT ChemFETs had n-type characteristics and were used as CO_2 gas sensors. The proposed sensing mechanism was as follows. Starch is hygroscopic and its presence will locally increase the amount of water. In the presence of water, the amine groups of the PEI can react with dissolved CO_2 to form carbamates. These introduce scattering centers that decrease the carrier mobility in the SWNTs, thereby increasing the electrical resistance. With this polymer CO_2 recognition layer, the functionalized SWNT ChemFET exhibited a high sensitivity, fast response time and complete reversibility for CO_2 concentrations ranging from 500 ppm to 10% in air. A straightforward manufacturing method was used by Lee and Strano [56]. They simply drop-casted either monomer or polymer solutions onto an SWNT mesh to produce non-covalently functionalized sensors. A systematic investigation of the effect of non-covalent functionalization with several amines such as aniline, ethylenediamine, pyridine, etc, revealed that the reversibility of the sensors to thionyl chloride vapors sensing was dependent on the amine basicity (pK_b) [56]. X-ray photoelectron spectroscopy (XPS) and molecular potential calculations demonstrated that the improved reversibility was due to the reduction of the binding energy of the analyte caused by the presence of the amine functional groups on the SWNTs. This effect was also observed when sensing two different organic vapors and therefore may be a general phenomenon.

Kuzmych *et al* developed ChemFET sensors based on PEI non-covalently functionalized SWNT networks to detect NO in exhaled breath [57]. The detection was based on the combination of an Ascarite scrubber (to remove the interference from CO_2), a CrO_3 converter (to oxidize NO to NO_2) and conductivity measurements. The polymer

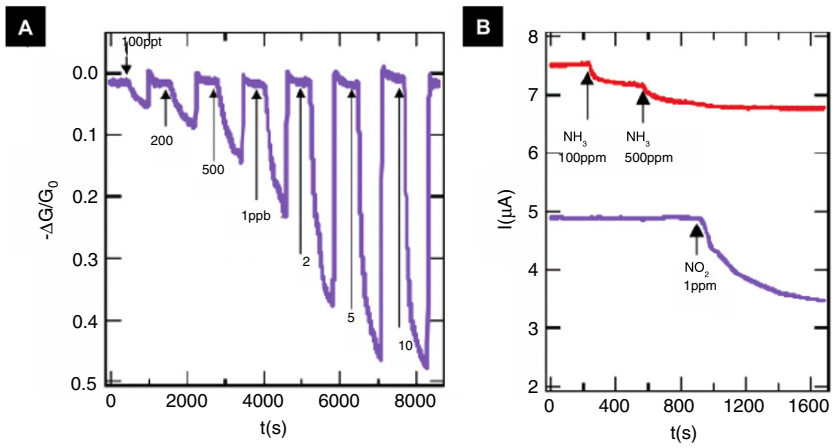

Figure 6. (A) Relative conductance response of a PEI-functionalized SWNT sensor to NO_2, demonstrating 100 ppt detection limit. The sensor recovery after NO_2 exposure was by UV illumination. (B) Top curve: a device coated with Nafion exhibits response to 100 and 500 ppm of NH_3 in air, and no response when 1 ppm of NO_2 was introduced into the environment. Bottom curve: a PEI-coated device exhibiting no response to 100 and 500 ppm of NH_3 and large conductance decrease to 1 ppm of NO_2. (Adapted with permission from Qi *et al* [33]. Copyright 2003 American Chemical Society.)

functionalization was achieved by drop-casting a PEI solution (10^{-3} M) onto a ChemFET device surface followed by drying. As in the case of Qi *et al* [33] mentioned above, PEI-coated ChemFET devices behaved as n-type transistors. The NO detection limit of the PEI-coated ChemFET was as low as 5 ppb in air at 30% relative humidity (RH), whereas that of a typical bare SWNT ChemFET was 300 ppb (gate voltage = 0 V). The response time was about 70 s for PEI-coated devices and 250 s for bare ChemFETs. The optimal RH for PEI-coated ChemFETs was between 15 and 30%, which the authors claim can be controlled by employing desiccants to decrease the RH to the desired level.

Bekyarova *et al* and Zhang *et al* demonstrated that chemically functionalized SWNTs with covalently attached poly-(m-aminobenzene sulfonic acid) (PABS) have better sensing performance for NH_3 and NO_2 than simple carboxylated SWNTs [58, 59]. The SWNT–PABS were synthesized by converting the carboxylic acid groups into an acyl chloride intermediate by treatment with oxalyl chloride, and subsequent reaction with an amine to give an amide [60] (figure 7). The sensing sensitivity toward NH_3 was greatly enhanced and a faster recovery time was observed. The improved sensing performance was attributed to the protonation–deprotonation of the functional group PABS which influenced the density of charge carriers in the SWNTs.

CNT/polymer nanocomposites also offer promising features as sensing materials. An *et al* fabricated SWNT/PPy nanocomposite-based gas sensors for NO_2 sensing [61]. The nanocomposites were prepared by a simple *in situ* chemical polymerization of pyrrole mixed with SWNTs to form a uniform coating of polypyrrole on SWNTs. The sensor was formed by spin-coating the nanocomposites onto prefabricated electrodes. The sensitivity of the nanocomposites was about ten times higher than that of polypyrrole (about 6% relative resistance change at 200 ppm NO_2). Abraham *et al* developed a wireless gas sensor using a MWNTs/PMMA composite film [62]. The composite solution was made by

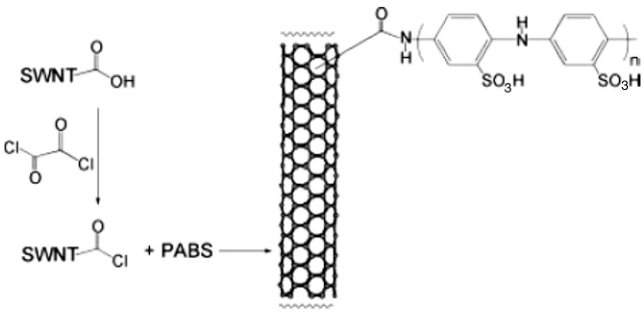

Figure 7. Synthesis of SWNT–PABS (source: Zhao *et al* [60]. Copyright Wiley-VCH Verlag GmbH & Co. KGaA. Reproduced with permission).

ultrasonication of MWNTs and PMMA (1:4 by weight) for 2 h in dichloromethane and the sensors were fabricated by dip-coating microfabricated electrodes in the solution followed by drying in air at 50 °C. The resistance changes of the sensor were wirelessly transmitted by a Bluetooth module to a notebook computer for data analysis. The sensor showed fast response time (2–5 s) and 100–1000-fold increase in resistance when exposed to saturated dichloromethane, chloroform and acetone vapors. The sensing mechanism was explained by swelling of the polymer due to absorption of organic vapors into the PMMA and the charge transfer when polar organic vapors adsorb on the CNT surface. Santhanam *et al* constructed similar poly(3-methylthiophene)/MWNT nanocomposite-based chemiresistors with *in situ* chemical polymerization of 3-methylthiophene [63]. The sensors were used to selectively discriminate between chloromethane and methane, as an increased resistance was observed upon exposure to chloromethane, while no response was observed when exposed to methane or many other VOCs. The sensing mechanism was proposed to be based on the ionization potential of the analytes. Wei *et al* developed novel multifunctional chemical sensors based on vertically aligned

MWNTs and polymer composites [64]. The sensors were fabricated by partially coating vertically aligned MWNTs with selected polymers (e.g. poly(vinyl acetate), polyisoprene) and sputtering gold electrodes. Rapid and reversible sensing of high concentrations of a variety of volatile organic solvents was demonstrated. The sensing mechanism was attributed to the charge transfer interaction with gas molecules and/or the inter-tube distance change induced by polymer swelling during gas adsorption.

In addition to chemical polymerization, electrochemical polymerization can be used to functionalize CNTs. Electrochemical polymerization is a simple technique which can offer site-specific functionalization of CNTs [65]. Since the process is electrochemically initiated, driven and terminated, the thickness, sometimes crystallinity, and morphology of coating layer or nanoparticles deposited can be precisely controlled by adjusting deposition time and applied potential. The electrical and materials properties can be tailored by controlling the solution composition (pH, monomer or metal ion concentration, supporting electrolytes, additives, complexing agents) and deposition parameters (current density, applied potential, temperature). Furthermore, electrochemical processes can be conducted at room temperature without complex equipment. Zhang *et al* recently demonstrated a facile method to make gas sensors using SWNTs electrochemically functionalized with PANI [65]. The sensitivity of the PANI–SWNT sensor to NH_3 was more than 60 times higher than carboxylated SWNT sensors. The detection limit was as low as 50 ppb_v, and good reproducibility upon repeated exposure to 10 ppm_v NH_3 was observed. The potential advantage of this fabrication method is that it enables targeted functionalization with different materials, thereby enabling manufacturing of high density individually addressable nanosensor arrays. Table 2 summarizes the sensing performance of selected polymer functionalized CNT sensors.

4.2. Metal nanoparticle/nanocluster functionalized CNT gas sensors

Metals exhibit a broad range of electronic, chemical and physical properties that are often highly sensitive to changes in their chemical environment [67]. They are mechanically and chemically robust and stable, and hence, compared to polymer-based sensors, metal-based sensors can operate at higher temperatures and in harsher environments. For example, elemental Pd and Pt are catalysts with high H_2 solubility and diffusivity, and good corrosion resistivity. They are widely used in hydrogen-related technologies such as fuel cell, batteries and H_2 sensors. Gold has been found to be sensitive to odorous gases containing thiol vapor and H_2S [68, 69].

Kong *et al* demonstrated room temperature H_2 sensors based on Pd nanoparticles (∼5 Å) deposited at the surface of SWNTs by electron-beam evaporation [70]. Pd-functionalized SWNTs were shown to be highly sensitive toward H_2, with a 50% greater sensitivity of up to 50% relative resistance change to 400 ppm H_2 for individual Pd-functionalized SWNTs compared to SWNT bundles. The response time was 5–10 s, and the time for recovery was about 400 s. The sensing mechanism was explained as follows: the adsorbed H_2 molecules are dissociated as hydrogen atoms, which dissolve into Pd with a high solubility, leading to a decrease in the work function of Pd. This causes electron transfer from Pd to SWNT and reduces the hole carriers in the p-type SWNT, and hence causes a decrease in conductance. The process is reversible as dissolved atomic hydrogen in Pd can combine with O_2 in air to form OH which will combine with atomic hydrogen to form water that can leave the Pd–SWNT system, thus recovering the sensor's initial conductance. The probable reactions that take place during hydrogen exposure and the recovery stage are as follows [70]:

Response:

$$H_{2,\text{in air}} \leftrightarrow 2H_{\text{on Pd surface}} \leftrightarrow 2H_{\text{on Pd–SWNT interface}}$$

Recovery:

$$2H_{\text{on Pd surface}} + O_2 \leftrightarrow 2(OH)_{\text{on Pd–SWNT interface}}$$

$$H_{\text{on Pd surface}} + (OH)_{\text{on Pd–SWNT interface}} \leftrightarrow H_2O.$$

Lu *et al* developed CH_4 sensors based on SWNTs loaded with Pd nanoparticles. The SWNTs were sputter-coated with a 10 nm thick layer of Pd, then mixed with other SWNTs [71]. The mixed Pd–SWNTs (∼1 wt%) were dispersed in water and the suspension was drop-casted on interdigitated electrodes to form a chemiresistive sensor. The fabricated sensors could detect low CH_4 concentrations (6–100 ppm), with enhanced sensitivity and reduced size and power consumption compared to conventional metal oxide sensors. A charge transfer sensing mechanism was proposed. Hydrogen atoms in CH_4 attract electrons from Pd, and electrons are withdrawn from the SWNT. This results in a weakly bound complex $Pd^{\delta+}(CH_4)^{\delta-}$, leaving more holes in the SWNTs, thereby increasing the conductance of p-type SWNTs when exposed to CH_4.

Sayago *et al* demonstrated two different methods for the functionalization of SWNTs with Pd to form H_2 sensors [72]. The first one consisted of a sidewall functionalization using SWNTs and a palladium salt using toluene as a solvent. TEM micrographs revealed uniform Pd nanoparticle (size: 3–10 nm) deposits on the outer surface of SWNT bundles. The second method consisted of sputtering Pd onto SWNT films. Pd-functionalized SWNTs were then deposited on alumina substrates by airbrushing Pd–SWNT dispersions to form the resistive sensors. The sensors all showed increased resistance when exposed to 0.1%–2% H_2 at room temperature. The chemically functionalized sensors were superior to the Pd-sputtered ones. Both the response time and the sensitivity decreased with increasing temperature. Interestingly, the sensors exhibited an improvement of their sensing properties (less cross-sensitivity, better reversibility) with aging of the sensors. This was attributed to unspecified structural and chemical changes over time.

Oakley *et al* made H_2 chemiresistors based on SWNT films coated with Pd [73]. Uniform SWNT films were prepared by vacuum filtering a diluted SWNT suspension through 0.1 μm pore size membrane filters. The thickness of the SWNT film deposited on the membrane could be controlled by the concentration of nanotubes and the volume of suspension filtered. The SWNT thin film was transferred onto a SiO_x/Si

Table 2. Summary of sensing performance of organic polymer functionalized CNT sensors. (Note: N/S = Not-stated.)

Organic polymer	CNT type	Sensor configuration	Targeted analytes	Functionalization method	Detection limit	Response time (s)	Reversibility	Reference
PEI, Nafion	SWNTs	ChemFET	NO_2, NH_3	Non-covalently drop-coating	100 ppt (NO_2)	60–120	Reversible (UV)	Qi *et al* [33]
PMMA	MWNTs	Chemiresistor	Dichloromethane, chloroform, acetone	Mixed as composite film	N/S	2–5	Reversible	Abraham *et al* [62]
PEI/Starch mixture	SWNTs	ChemFET	CO_2	Non-covalently dip-coating	500 ppm	60	Reversible	Star *et al* [55]
PEI	SWNTs	ChemFET	NO	Non-covalently drop-coating	5 ppb	70	Reversible	Kuzmych *et al* [57]
Polypyrrole	SWNTs	ChemFET	NO_2	Covalent chemical polymerization	N/S	600–1800	Reversible	An *et al* [61]
Poly(3-methylthiophene)	MWNTs	Chemiresistor	CH_2Cl_2, $CHCl_3$, CCl_4, CH_4	Covalent chemical polymerization	N/S	60–120	Reversible	Santhanam *et al* [63]
PABS	SWNTs	Chemiresistor	NH_3, NO_2, H_2O	Covalent chemical functionalization	20 ppb (NO_2), 100 ppb (NH_3)	600	Reversible	Zhang *et al* [59]
Poly(vinyl acetate), Polyisoprene	MWNTs	Chemiresistor	Tetrahydrofuran, ethanol, cyclohexane	Non-covalently drop-coating	N/S	1200	Reversible	Wei *et al* [64]
Polyaniline	SWNTs	Chemiresistor	NH_3	Non-covalent electrochemical functionalization	50 ppb	600	Reversible	Zhang *et al* [65]
Polyaniline	MWNTs	Chemiresistor	Triethylamine	*In situ* polymerization (PANI–SWNT composite)	500 ppb	200–400 (up to 600 for recovery)	Reversible	Li *et al* [66]

substrate, followed by sputtering ~50 nm thick Pd pads to form electrical contacts. Functionalization of SWNT was achieved by sputtering a 1–3 nm thick layer of Pd across the entire SWNT film. The Pd-coated SWNT film could detect 10 ppm H_2 at room temperature and relative resistance changes were about 20% for 100 ppm H_2 and 40% for 500 ppm H_2. In most cases, the initial resistance of the sensor was recovered within 30 s when exposed back to air.

Young *et al* fabricated NO_2 sensors based on Au–SWNT nanoparticle composite films [74]. A SWNT mesh was doped with alkanethiol-monolayer-protected gold clusters (MPCs) resulting in a composite film that was then used for the chemiresistive sensing of low concentrations of NO_2 under ambient conditions. The sensitivity of the sensors was dependent on the loading of MPCs, which decreased the detection limit for NO_2 approximately tenfold, to 4.6 ppb, compared with that obtained with SWNT-only sensors. Illumination with ultraviolet radiation accelerated the recovery after exposure to the target analyte.

Kumar *et al* demonstrated that MWNTs chemically functionalized with Pt and Pd were good H_2 sensors at room temperature [75]. Purified and chemically treated MWNTs were functionalized by using solutions of H_2PtCl_6 or $PdCl_2$ and adding reducing agents such as $NaBH_4$, resulting in Pt or Pd nanoparticle formation on the MWNTs. The nature of the nanostructures was confirmed by elemental analysis using energy-dispersive spectroscopy (EDS). Systematic investigations of hydrogen sensing properties of the Pd- or Pt–MWNT ensembles were carried out. They showed high sensitivity and reversibility at room temperature. The sensing mechanism is expected to similar to that of Pd–CNTs explained above.

Mubeen *et al* developed a simple electrochemical functionalization method to fabricate a H_2 nanosensor by site-specific electrodeposition of Pd nanoparticles on SWNTs (figure 8) [76]. Optimal sensing performance was obtained by varying the sensor's synthesis conditions (e.g. Pd electrodeposition charge, deposition potential and initial baseline resistance of the SWNT network). The optimized sensor showed good sensitivity toward H_2 (0.42% resistance change per ppm) with a detection limit of 100 ppm and a linear response up to 1000 ppm at room temperature. The sensor response was not reversible for H_2 sensing in argon, while the recovery was shortened in humid air compared to dry air conditions, indicating an important role for water in the sensor dynamics.

Penza *et al* demonstrated Au and Pt nanocluster functionalized MWNT chemiresistors for NO_2 and NH_3 gas sensing at high temperature (100–250 °C) [77]. MWNTs were synthesized by plasma-enhanced CVD onto Cr–Au patterned alumina substrates, provided with 3 nm thick Fe growth catalyst. Au (6–20 nm) and Pt (6–60 nm) nanoclusters were then sputtered on the surface of MWNTs. The authors found that the sensitivity of Pt- and Au-functionalized MWNTs towards NH_3 and NO_2 improved by one order of magnitude.

Metal nanoparticle functionalized CNT sensor arrays have also been demonstrated. Star *et al* fabricated ChemFET arrays on a single Si chip by site-selective electrochemical functionalization of isolated SWNT networks with different catalytic metal nanoparticles (Au, Pt, Pd, Rh, etc) [78]. The differences in catalytic activities of the metal nanoparticles caused different selectivities for the detection of H_2, CH_4, CO, H_2S, NH_3 and NO_2. The output of the sensor array was analyzed using principal component analysis (PCA) and partial least squares regression (PLS) in order to identify the above-mentioned gases. Lu *et al* demonstrated a gas sensor array composed of 32 sensing elements with pristine, metal-doped and polymer-coated SWNTs for discriminating gases such as NO_2, HCN, HCl, Cl, acetone and benzene at ppm concentration levels [79]. The sensor array data was also analyzed with PCA and successfully discriminated the targeted gases.

Sun and Wang fabricated H_2 sensors based on electrodeposition of Pd nanoparticles on SWNTs on a flexible plastic substrate [80]. The fabrication procedure was as follows: as-grown SWNTs were first transferred onto an insulating plastic polyethylene terephthalate (PET, coated with epoxy resin as an adhesive layer) coupon by an elastomeric polydimethylsiloxane (PDMS) stamping technique. A thin Au layer was deposited on one end of the SWNT network to serve as the electrode, and Pd nanoparticles were electrodeposited onto the SWNT network using a three-electrode configuration and a potentiostatic mode (−1.0 V). The Pd-functionalized SWNT flexible sensors could readily detect 100 ppm H_2 (with 5% relative response) at room temperature. The response time for 37% of the steady state resistance change was in the range of a few seconds up to 1 min, or close to 5 min to reach a value close to steady state. The mechanical bendability of the flexible sensors was proved to have negligible effect (<5%) on the sensing performance. Table 3 summarizes the sensing performance of selected metal nanoparticle/nanocluster functionalized CNT sensors.

5. Conclusion

Recent research and development of CNT-based gas sensors were reviewed. CNTs have a large surface-to-volume ratio and unique electrical properties, which make them some of the most promising materials for the development of the next generation of chemical gas sensors. To overcome some of the limitations posed by pristine CNT sensors, researchers have directed their efforts toward the functionalization of CNTs with various methods and with a wide spectrum of materials such as conducting polymers and metal nanoparticles. Functionalized CNT sensors often offer a higher sensitivity and a better selectivity compared to pristine CNT sensors. The broad variety of functionalization techniques together with the choice of functional materials that can be deposited make functionalized CNTs some of the most exciting building blocks for miniaturized gas sensors and high density gas sensor arrays. Even so, challenges for the realization of commercially viable devices are numerous. They include the development of a detailed fundamental understanding

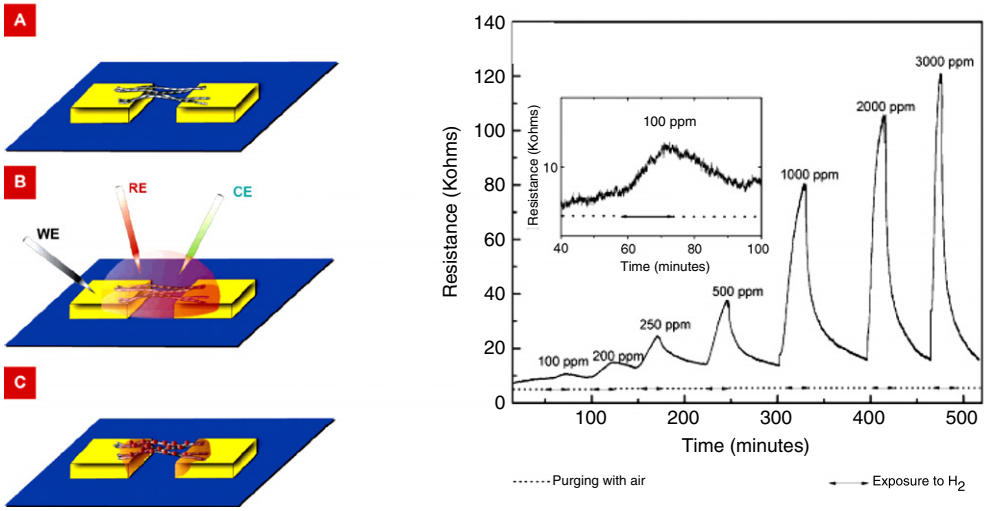

Figure 8. Left: Schematic of the electrochemical synthesis method for Pd–SWNT. (A) SWNTs are deposited across the electrodes. (B) Electrochemical functionalization of the SWNTs (WE: working electrode; CE: counter electrode; RE: reference electrode). (C) Pd nanoparticles formed on SWNTs. Right: a Pd–SWNT sensor response to different concentrations of H_2 in 80% relative humidity air. (Adapted from Mubeen *et al* [76]. Copyright 2007 American Chemical Society.)

Table 3. Summary of sensing performance of metal functionalized CNT sensors. (Note: N/S = Not-stated.)

Metal	CNT type	Sensor configuration	Targeted gas/vapor	Functionalization method	Detection limit	Response time (s)	Reversibility	Ref
Pd	Single SWNT	ChemFET	H_2	Electron-beam evaporation	<40 ppm	5–10 (for half resistance change)	Reversible	Kong *et al* [70]
Pd	SWNTs	Chemiresistor	CH_4	Sputter-coating	6 ppm	120–240	Reversible (UV)	Lu *et al* [71]
Pd	SWNTs	Chemiresistor	H_2	(1) Chemical functionalization, (2) Sputter-coating	1000 ppm	N/S	Reversible	Sayago *et al* [72]
Pd	SWNTs	Chemiresistor	H_2	(1) Thermal evaporation (2) Sputtered coating	~10 ppm	<600	Reversible	Oakley *et al* [73]
Au, Pt	MWNTs	Chemiresistor	NO_2, NH_3	Sputter-coating	100 ppb (NO_2), 5 ppm (NH_3)	<600	Reversible (150 °C)	Penza *et al* [77]
Au	SWNTs	Chemiresistor	NO_2	Drop-coating monolayer Au clusters	4.6 ppb	N/S	Reversible (UV)	Young *et al* [74]
Pt, Pd	MWNTs	Chemiresistor	H_2, NO_2, H_2O	Chemical functionalization	N/S	600–1800	Reversible	Kumar *et al* [75]
Pd	SWNTs	Chemiresistor	H_2	Electrochemical functionalization	100 ppm	600	Reversible	Mubeen *et al* [76]
Pt, Pd, Sn, Rh	SWNTs	ChemFET	H_2, CH_4, CO, H_2S	(1) Electrochemical functionalization (2) Electron-beam evaporation	N/S	600	Reversible	Star *et al* [78]
Pd	SWNTs	Chemiresistor	H_2	Electrochemical functionalization	100 ppm	3–60 (for 36.8% resistance change)	Reversible	Sun and Wang [80]

of the sensing mechanisms of these novel sensors and the utilization of this information for the rational design of nanostructured sensing materials, the development of analyte-specific, fast and stable sensors and sensor arrays together with appropriate numerical methods to analyze sensor array data, and the development of suitable high throughput nanomanufacturing techniques that enable mass production of high density sensor arrays. While much progress has been done recently in these areas, commercial success of CNT-based gas sensing will only be realized when dealing with these challenges becomes routine and adequate technology transfer has occurred.

Acknowledgments

We greatly acknowledge the support for our gas sensor research by NIH-NIEHS (Gene-Environment Initiative, grant U01ES016026), Bourns, Inc. and the University of California Discovery Program (UC Discovery) and DOD/DMEA through the Center for Nanoscience Innovation for Defense (grant no. DOD/DMEA-H94003-06-2-0608).

References

[1] Kolmakov A and Moskovits M 2004 *Annu. Rev. Mater. Res.* **34** 151–80
[2] Iijima S 1991 *Nature* **354** 56–8
[3] Ajayan P M and Zhou O Z 2001 *Carbon Nanotubes* **391** 425
[4] Baughman R H, Zakhidov A A and de Heer W A 2002 *Science* **297** 787–92
[5] Dresselhaus M S and Dai H 2004 *MRS Bull.* **29** 237–9
[6] Dai H J 2002 *Surf. Sci.* **500** 218–41
[7] Meyyappan M 2005 *Carbon Nanotubes: Science and Applications* (Boca Raton, FL: CRC Press) p 214
[8] Dresselhaus M S, Dresselhaus G and Eklund P C 1996 *Science of Fullerenes and Carbon Nanotubes* (San Diego, CA: Academic)
[9] Antisari M V, Marazzi R and Krsmanovic R 2003 *Carbon* **41** 2393–401
[10] Arepalli S 2004 *J. Nanosci. Nanotechnol.* **4** 317–25
[11] Braidy N, El Khakani M A and Botton G A 2002 *J. Mater. Res.* **17** 2189–92
[12] Choi Y C, Bae D J, Lee Y H, Lee B S, Park G S, Choi W B, Lee N S and Kim J M 2000 *J. Vac. Sci. Technol.* A **18** 1864–8
[13] Ebbesen T W and Ajayan P M 1992 *Nature* **358** 220–2
[14] Wei B Q, Vajtai R and Ajayan P M 2001 *Appl. Phys. Lett.* **79** 1172–4
[15] Treacy M M J, Ebbesen T W and Gibson J M 1996 *Nature* **381** 678–80
[16] Zhang W, Zhu Z Y, Wang F, Wang T T, Sun L T and Wang Z X 2004 *Nanotechnology* **15** 936–9
[17] Hone J, Llaguno M C, Nemes N M, Johnson A T, Fischer J E, Walters D A, Casavant M J, Schmidt J and Smalley R E 2000 *Appl. Phys. Lett.* **77** 666–8
[18] Martel R, Schmidt T, Shea H R, Hertel T and Avouris P 1998 *Appl. Phys. Lett.* **73** 2447–9
[19] Dai H J 2001 *Carbon Nanotubes* (Springer: Berlin)
[20] Sun Y P, Fu K, Lin Y and Huang W 2002 *Acc. Chem. Res.* **35** 1096–104
[21] Kong J, Franklin N R, Zhou C W, Chapline M G, Peng S, Cho K J and Dai H J 2000 *Science* **287** 622–5
[22] Someya T, Small J, Kim P, Nuckolls C and Yardley J T 2003 *Nano Lett.* **3** 877–81
[23] Collins P G, Bradley K, Ishigami M and Zettl A 2000 *Science* **287** 1801–4
[24] Novak J P, Snow E S, Houser E J, Park D, Stepnowski J L and McGill R A 2003 *Appl. Phys. Lett.* **83** 4026–8
[25] Chang Y W, Oh J S, Yoo S H, Choi H H and Yoo K H 2007 *Nanotechnology* **18** 435504
[26] Valentini L, Cantalini C, Armentano I, Kenny J M, Lozzi L and Santucci S 2003 *J. Vac. Sci. Technol.* B **21** 1996–2000
[27] Li J, Lu Y J, Ye Q, Cinke M, Han J and Meyyappan M 2003 *Nano Lett.* **3** 929–33
[28] Suehiro J, Zhou G B and Hara M 2003 *J. Phys. D: Appl. Phys.* **36** 109–14
[29] Lee C Y, Baik S, Zhang J Q, Masel R I and Strano M S 2006 *J. Phys. Chem.* B **110** 11055–61
[30] Kordás K, Mustonen T, Tóth G, Jantunen H, Lajunen M, Soldano C, Talapatra S, Kar S, Vajtai R and Ajayan P M 2006 *Small* **2** 1021–5
[31] Wongwiriyapan W *et al* 2006 *Japan. J. Appl. Phys.* **45** 3669–71
[32] Bradley K, Gabriel J C P, Briman M, Star A and Gruner G 2003 *Phys. Rev. Lett.* **91** 218301–4
[33] Qi P F, Vermesh O, Grecu M, Javey A, Wang O, Dai H J, Peng S and Cho K J 2003 *Nano Lett.* **3** 347–51
[34] Chen R J, Franklin N R, Kong J, Cao J, Tombler T W, Yhang Y and Dai H 2001 *Appl. Phys. Lett.* **79** 2258–60
[35] Valentini L, Mercuri F, Armentano I, Cantalini C, Picozzi S, Lozzi L, Santucci S, Sgamellotti A and Kenny J M 2004 *Chem. Phys. Lett.* **387** 356–61
[36] Robinson J A, Snow E S, Badescu S C, Reinecke T L and Perkins F K 2006 *Nano Lett.* **6** 1747–51
[37] Watts P C P, Mureau N, Tang Z N, Miyajima Y, Carey J D and Silva S R P 2007 *Nanotechnology* **18** 175701–6
[38] Peng S and Cho K 2003 *Nano Lett.* **3** 513–7
[39] Wang R, Zhang D, Sun W, Han Z and Liu C 2007 *J. Mol. Struct. (Theochem)* **806** 93–7
[40] Fu D, Lim H, Shi Y, Dong X, Mhaisalkar S G, Chen Y, Moochhala S and Li L J 2008 *J. Phys. Chem.* C **112** 650–3
[41] Snow E S, Perkins F K, Houser E J, Badescu S C and Reinecke T L 2005 *Science* **307** 1942–5
[42] Snow E S and Perkins F K 2005 *Nano Lett.* **5** 2414–7
[43] Modi A, Koratkar N, Lass E, Wei B Q and Ajayan P M 2003 *Nature* **424** 171–4
[44] Chopra S, Pham A, Gaillard J, Parker A and Rao A M 2002 *Appl. Phys. Lett.* **80** 4632–4
[45] Ong K G, Zeng K and Grimes C A 2002 *IEEE Sensors* **2** 82–8
[46] Penza M, Cassano G, Aversa P, Cusano A, Cutolo A, Giordano M and Nicolais L 2005 *Nanotechnology* **16** 2536–47
[47] Chen J, Hamon M A, Hu H, Chen Y, Rao A M, Eklund P C and Haddon R C 1998 *Science* **282** 95–8
[48] Hamon M A, Hu H, Bhowmik P, Niyogi S, Zhao B, Itkis M E and Haddon R C 2001 *Chem. Phys. Lett.* **347** 8–12
[49] Riggs J E, Guo Z, Carroll D L and Sun Y P 2000 *J. Am. Chem. Soc.* **122** 5879–80
[50] Star A, Stoddart J F, Steuerman D, Diehl M, Boukai A, Wong E W, Yang X, Chung S W, Choi H and Heath J R 2001 *Angew. Chem.* **113** 1771–5
[51] Xia H, Wang Q and Qiu G 2003 *Chem. Mater.* **15** 3879–86
[52] Dong X, Fu D, Ahmed M O, Shi Y, Mhaisalkar S G, Zhang S, Moochhala S, Ho X, Rogers J A and Li L J 2007 *Chem. Mater.* **19** 6059–61
[53] Osada Y and Rossi D E 2000 *Polymer Sensors and Actuators* (Berlin: Springer)
[54] Janata J and Josowicz M 2003 *Nat. Mater.* **2** 19–24
[55] Star A, Han T R, Joshi V, Gabriel J C P and Gruner G 2004 *Adv. Mater.* **16** 2049–52
[56] Lee C Y and Strano M S 2008 *J. Am. Chem. Soc.* **130** 1766–73
[57] Kuzmych O, Allen B L and Star A 2007 *Nanotechnology* **18** 375502
[58] Bekyarova E, Davis M, Burch T, Itkis M E, Zhao B, Sunshine S and Haddon R C 2004 *J. Phys. Chem.* B **108** 19717–20
[59] Zhang T, Mubeen S, Bekyarova E, Yoo B Y, Haddon R C, Myung N V and Deshusses M A 2007 *Nanotechnology* **18** 165504–9
[60] Zhao B, Hu H and Haddon R C 2004 *Adv. Funct. Mater.* **14** 71–6
[61] An K H, Jeong S Y, Hwang H R and Lee Y H 2004 *Adv. Mater.* **16** 1005–9
[62] Abraham J K, Philip B, Witchurch A, Varadan V K and Reddy C C 2004 *Smart Mater. Struct.* **13** 1045–9
[63] Santhanam K S V, Sangoi R and Fuller L 2005 *Sensors Actuators* B **106** 766–71
[64] Wei C, Dai L, Roy A and Tolle T B 2006 *J. Am. Chem. Soc.* **128** 1412–3

[65] Zhang T, Nix M B, Yoo B Y, Deshusses M A and Myung N V 2006 *Electroanalysis* **18** 1153–8
[66] Li Y, Wang H, Cao X, Yuan M and Yang M 2008 *Nanotechnology* **19** 015503
[67] Ruiz A, Arbiol J, Cirera A, Cornet A and Morante J R 2002 *Mater. Sci. Eng.* C **19** 105–9
[68] Lewis F A 1967 *Palladium Hydrogen System* (New York: Academic)
[69] Galipeau J D, Falconer R S, Vetelino J F, Caron J J, Wittman E L, Schweyer M G and Andle J C 1995 *Sensors Actuators* B **24** 49–53
[70] Kong J, Chapline M G and Dai H J 2001 *Adv. Mater.* **13** 1384–6
[71] Lu Y J, Li J, Han J, Ng H T, Binder C, Partridge C and Meyyappan M 2004 *Chem. Phys. Lett.* **391** 344–8
[72] Sayago I *et al* 2007 *Sensors Actuators* B **122** 75–80
[73] Oakley J S, Wang H T, Kang B S, Wu Z, Ren F, Rinzler A G and Pearton S J 2005 *Nanotechnology* **16** 2218–21
[74] Young P, Lu Y J, Terrill R and Li J 2005 *J. Nanosci. Nanotechnol.* **5** 1509–13
[75] Kumar M K and Ramaprabhu S 2006 *J. Phys. Chem.* B **110** 11291–8
[76] Mubeen S, Zhang T, Yoo B, Deshusses M A and Myung N V 2007 *J. Phys. Chem.* C **111** 6321–7
[77] Penza M, Cassano G, Rossi R, Alvisi M, Rizzo A, Signore M A, Dikonimos T, Serra E and Giorgi R 2007 *Appl. Phys. Lett.* **90** 171231–3
[78] Star A, Joshi V, Skarupo S, Thomas D and Gabriel J C P 2006 *J. Phys. Chem.* B **110** 21014–20
[79] Lu Y J, Partridge C, Meyyappan M and Li J 2006 *J. Electroanal. Chem.* **593** 105–10
[80] Sun Y and Wang H H 2007 *Appl. Phys. Lett.* **90** 213107